# Morphogenetic Control of Calcite Crystal Growth in Sulfonic Acid Based Hydrogels

**Olaf Grassmann and Peer Löbmann*[a]**

**Abstract:** In this paper the mineralization of $CaCO_3$ in various hydrogel matrices is presented. Sulfonic acid based hydrogels were prepared by introduction of sulfonate-containing monomers into a polyacrylamide network. The sulfonate content of polyacrylamide-*co*-vinylsulfonate and polyacrylamide-*co*-allylsulfonate decreases during elution of the copolymers in demineralized water, indicating insufficient linking of the sulfonate-bearing monomers within the hydrogel. In contrast to this, acrylamidomethylpropanesulfonate (AMPS) effectively copolymerizes with acrylamide (AAm) monomers. To study the influence of spatial arrangement of ionic functional groups within hydrogel networks on the mineralization of $CaCO_3$, AMPS copolymers with different degrees of AMPS cross-linking were synthesized. For the mineralization experiments the copolymers were placed into a double-diffusion arrangement. Calcite as the thermodynamically stable modification of $CaCO_3$ was obtained with a particular morphology. The pseudocubic habitus resembles aggregates obtained by mineralization in pure polyacrylamide. However, closer examination of the aggregates by scanning electron microscopy (SEM) shows that the crystal growth in the AMPS copolymers is different from that observed in polyacrylamide. Whereas the morphology of the calcite aggregates could be fine-tuned by using copolymers with different sulfonate content, the spatial distribution of the ionic functional groups alters the course of crystallization. Calcium ions are locally accumulated due to the heterogeneous distribution of functional sulfonate groups within the copolymer network. Thereby the nucleation of calcite is triggered, resulting in enhanced mineralization.

**Keywords:** biomineralization · calcite · copolymerization · crystal growth · double diffusion

## Introduction

In biological systems deposition of inorganic materials commonly takes place in gel-like extracellular matrices.[1] The mineralization of human bone and aragonite layers of nacre is governed by complex protein-mediated processes. Matrix macromolecules from shell nacre are characterized by two different sets of proteins:[2] acidic macromolecules containing carboxylate groups are adsorbed onto a scaffold of silk-fibroin-like proteins. Whereas the uncharged framework molecules provide the physical environment for crystallization, the acidic macromolecules, rich in aspartate and glutamate side groups, promote the nucleation of the inorganic $CaCO_3$ phase.[3] Since these processes take place at ambient temperature and the resulting biominerals show remarkable mechanical properties,[4] biomimetic deposition processes are promising for technical applications.

For preparing $TiO_2$ coatings on silicon substrates a biologically inspired approach has been employed. Highly ionic, sulfonic acid containing silanes self assemble on a substrate, leading to organized monolayers with acidic terminal groups. It was observed that the deposition of $TiO_2$ on these functionalized substrates is modified resulting in partially crystalline coatings.[5] SAMs (SAM = self-assembled monolayer) with $-SO_3^-$ end groups on metal surfaces induce the nucleation of calcite better than bare metal films.[6] So far it is still debated whether biomimetic crystallization is mediated through an epitactical match of acidic head groups and the inorganic phase or solely by the presence of charged functionalities.[7, 8] According to the ionotropic model of nucleation[9] the spatial distribution of polar functional groups, that is, the local charge density, is of crucial importance for the nucleation.

To compare the effect of highly polar groups in a system more closely related to nature than SAMs, we study the crystallization of $CaCO_3$ within a functionalized hydrogel network. For that pupose, sulfonic acid containing monomers are copolymerized with acrylamide monomers to provide a model system for demonstrating the principles of biomineralization. In this paper we describe the synthesis of sulfonic acid containing copolymers with varying degrees of steric restriction of the sulfonate groups. $CaCO_3$ is precipitated within the functionalized hydrogels by means of a counter-

[a] Dr. P. Löbmann, O. Grassmann
Lehrstuhl für Silicatchemie, Universität Würzburg
Röntgenring 11, 97070 Würzburg (Germany)
Fax: (+49) 931-31-21-09
E-mail: loebmann@silchem.uni-wuerzburg.de

  0947-6539/03/0906-1310 $ 20.00+.50/0 

diffusion arrangement. The effect of the hydrogel matrix on the crystallization is analyzed and compared to the deposition within an unmodified polyacrylamide hydrogel network.

## Results and Discussion

**Synthesis of sulfonic acid based hydrogels**: To evaluate the influence of sulfonate groups on the crystallization of $CaCO_3$ it is crucial to quantify the efficiency of copolymerization, that is, the proportion of covalently linked sulfonate containing monomers within the hydrogel network. Incubation of the copolymers in demineralized water will elute monomers not covalently bonded to the hydrogel network by diffusion following the concentration gradient. For that reason, the amount of sulfur within the hydrogels is an indicator for the degree of copolymerization. Thus copolymers characterized by a sulfur content of the eluted samples, corresponding to the theoretical (as-synthesized) amount, show efficient copolymerization. The molar ratio of sulfonate groups within these hydrogel networks is adjustable.

To synthesize sulfonic acid based hydrogels three different types of sulfonate-containing monomers were employed: sodium vinylsulfonate (VlS), sodium allylsulfonate (AlS) and sodium 2-acrylamido-2-methyl-1-propanesulfonate (AMPS). In order to investigate the degree of copolymerization, the $-SO_3^-$-bearing monomers were copolymerized in various mole fractions. In Figure 1 the theoretical sulfur

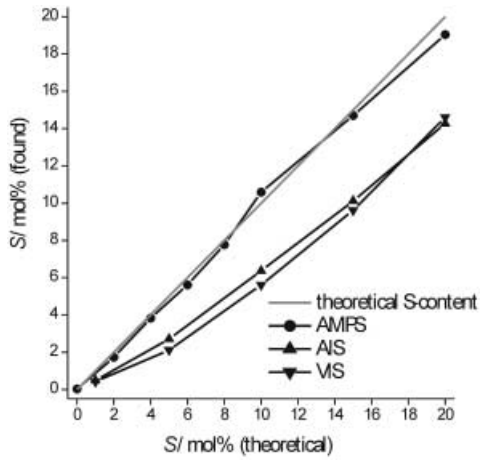


Figure 1. Sulfur content of AlS, VlS and AMPS copolymers determined by XRF. The sulfur content of eluted AMPS copolymers corresponds to the theoretical sulfur content.

content of VlS, AlS, and AMPS that corresponds to the synthesis is compared with the sulfur content of eluted samples. The molar ratio of sulfur within the eluted VlS and AlS copolymers deviates significantly from the theoretical values. Increasing the amount of sulfonate-containing monomers within the hydrogels leads to a pronounced discrepancy to the theoretical sulfur content, indicating a distinctive elution effect during incubation. The insufficient copolymerization of acrylamide (AAm) with AlS is in agreement with different reactivity ratios of the monomers determined by the Kelen–Tudos method.[12] The AMPS copolymers, however, show a molar sulfur ratio that closely corresponds to the theoretical amount. Thus the AMPS monomers are suitable components for the synthesis of sulfonic acid based hydrogels.

Since the ratio, in the IR spectrum, of the absorption peak of the SO group (1040 $cm^{-1}$) and the C=O stretching peak (1660 $cm^{-1}$) is characteristic for the amount of AMPS monomers within a hydrogel,[13] samples were analyzed by IR spectroscopy. Figure 2 (top) shows a typical IR spectrum of an

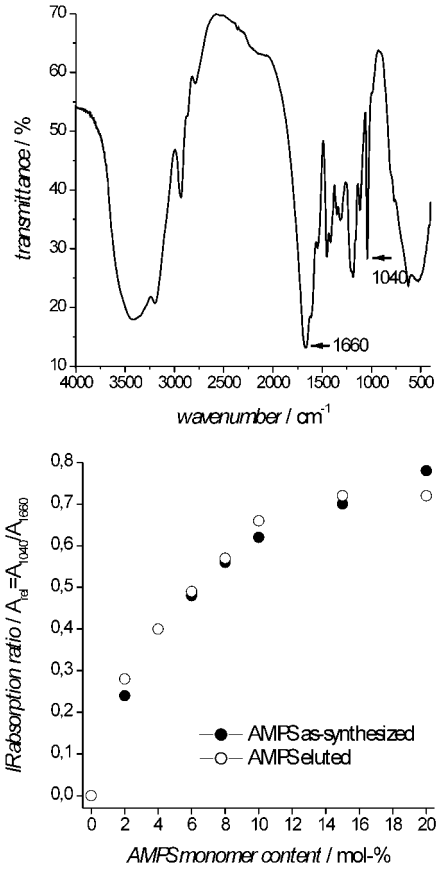


Figure 2. IR spectroscopy of AMPS copolymers: typical IR spectrum of a 10 mol-% sulfonate monomer containing copolymer (top), IR absorption ratio $A_{rel} = A_{1040}/A_{1660}$(bottom).

AAm-AMPS copolymer with 10 mol% AMPS relative to the AAm monomers. At 1040 $cm^{-1}$ the SO absorption peak is clearly visible. An absorption peak at 1660 $cm^{-1}$ corresponds to the C=O stretching peak of AAm and AMPS units. The absorption band around 3450 $cm^{-1}$ is due to moisture of the hygroscopic potassium bromide. To quantify the AMPS content within the copolymers the intensity of the characteristic absorption peak of AMPS is normalized by using the C=O stretching peak. In Figure 2 (bottom) the ratio $A_{rel} = A_{1040}/A_{1660}$ for as-synthesized and eluted hydrogels is shown. The absorption ratio of the eluted samples only slightly deviates from the as-synthesized hydrogels. This efficient copolymerization of AAm and AMPS has already been shown in previous studies,[13] and the results of the sulfur analysis determined by X-ray fluorescence analysis (XRF) are confirmed. It is possible to adjust the content of $-SO_3^-$ groups within a hydrogel network by using AMPS monomers.

  0947-6539/03/0906-1311 $ 20.00+.50/0 

Consequently, AAm-AMPS copolymers are suitable growth environments to analyze the effect of polar functional groups on the biomimetic mineralization of $CaCO_3$.

To investigate the effect of the spatial distribution of functional groups within a hydrogel network on biomimetic mineralization, the AAm-AMPS copolymer synthesis was modified so as to regulate the spatial distribution of AMPS monomers within the network. Local accumulation of AMPS is achieved by prepolymerization of the monomers. After addition of the radical starter to a solution of AMPS and cross-linker the monomers locally polymerize. Since the gelation time of pure poly-AMPS hydrogels exceeds the time of one hour,[14] it is possible to synthesize poly-AAm-AMPS copolymers by pouring the prepolymerization solution into a solution of AAm monomers. The prepolymerization of AMPS is altered by the amount of cross-linker present. It is expected that weakly AMPS-cross-linked hydrogels (AMPS-2) are generally characterized by linear polymerization of AMPS monomers. During prepolymerization the cross-linker content of highly AMPS-cross-linked copolymers (AMPS-3) is by an order of magnitude higher; this leads to cross-linked AMPS clusters. The supposed topography of the various copolymers is illustrated in Figure 3. The limiting factor of the degree of AMPS cross-linking is the insufficient solubility of MBAAm in water. Since for the synthesis of strongly cross-linked copolymers the *N*,*N*′-methylenbis(acrylamide) (MBAAm) monomers are very concentrated within the prepolymerization solution, the maximum mole fraction of AMPS within these copolymers is restricted to 10 mol%.

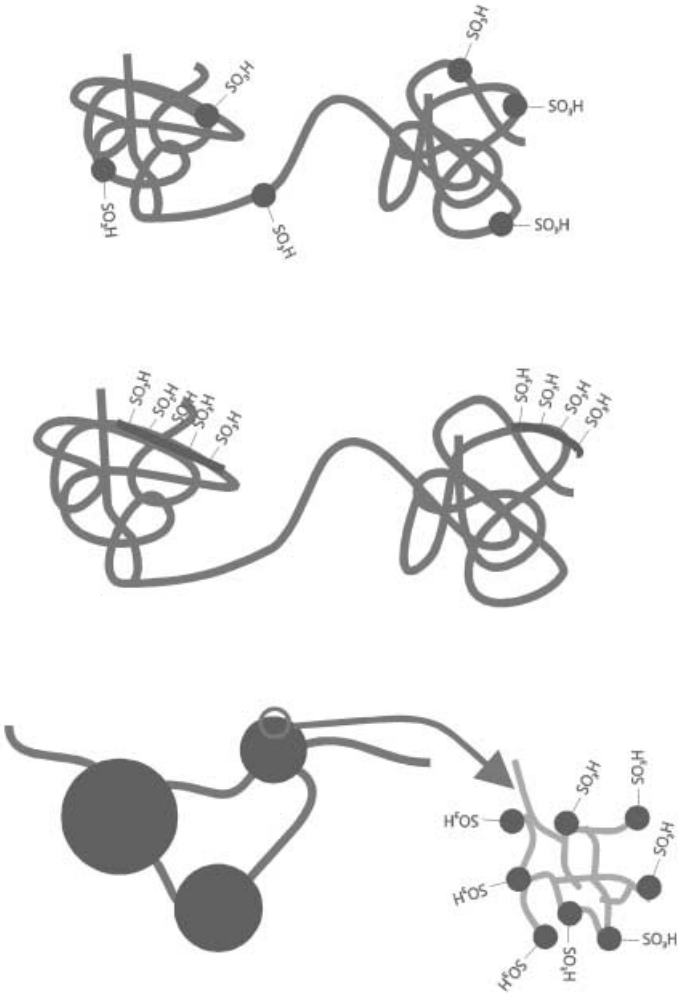


Figure 3. Illustration of the supposed spatial arrangement of functional groups in various AMPS copolymers: random distribution of functional groups (top), weakly AMPS-cross-linked copolymers (middle), and highly AMPS-cross-linked copolymers (bottom).

**Copolymer swelling**: According to Flory,[15] the equilibrium swelling is determined by compensation of the potential differences between a polymer and the swelling solution. Essential parameters affecting the swelling are the osmotic pressure, due to polar groups within the hydrogel, and the elastic properties of the network. The osmotic pressure has to be compensated by the repulsive force inherent to the network. For hydrogels with a physical density comparable to the swelling solution, the degree of swelling is sufficiently approximated by the weight swelling ratio $Q_w = m_q/m_0$, in which $m_q$ and $m_0$ are the weight of the swollen samples and the weight of the unswollen hydrogel, respectively.[16]

The spatial arrangement of polar functional groups within the synthesized hydrogels is estimated by comparison of the swelling behaviour. It is expected that a statistical distribution of AMPS moieties (AMPS-1) will result in the highest relative swelling ratios. In contrast to the AMPS-cross-linked copolymers the hydrate shells surrounding the polar functional groups should not hinder each other. Analogously, highly AMPS-cross-linked hydrogels should be characterized by a less pronounced osmotic pressure. The swelling ratios of the different hydrogels in relation to the mole fraction of AMPS monomers are shown in Figure 4 (top). For 5 and 10 mol% AMPS the statistical copolymer is characterized by the highest relative swelling ratios. Weakly AMPS-cross-linked (AMPS-2) copolymers show the smallest swelling ratios, whereas the swelling behaviour of highly AMPS-cross-linked (AMPS-3) copolymers is intermediate. Since the overall cross-linker concentration of the different copolymer types is identical, less cross-linker is available for bulk polymerization of AMPS-3 relative to AMPS-2. Because of the local clustering of the cross-linker, the AMPS-3 copolymers are expected to show less stiffness of the bulk network.

To evaluate the effect of the cross-linker content on the hydrogel swelling ratio, statistical copolymers with different AAm-AMPS/cross-linker ratios were synthesized. The swelling ratios of the AMPS-1 gels are clearly dependent on the AAm-AMPS/cross-linker ratio. Copolymers with a monomer : cross-linker ratio of 19:1 swell significantly less than copolymers with a ratio of 29:1 (Figure 4, bottom). Thus, it has to be taken into account that highly AMPS-cross-linked (AMPS-3) gels are characterized by a relatively low swelling ratio despite the small cross-linker content of the bulk hydrogel network. Consequently, the swelling behavior is determined by two opposing effects: reduction of the swelling ratio due to the hindering of $-SO_3^-$ groups and an increased swelling because of inhomogeneous distribution of cross-linker.



0947-6539/03/0906-1312 $ 20.00+.50/0 *Chem. Eur. J.* **2003**, *9*, No. 6

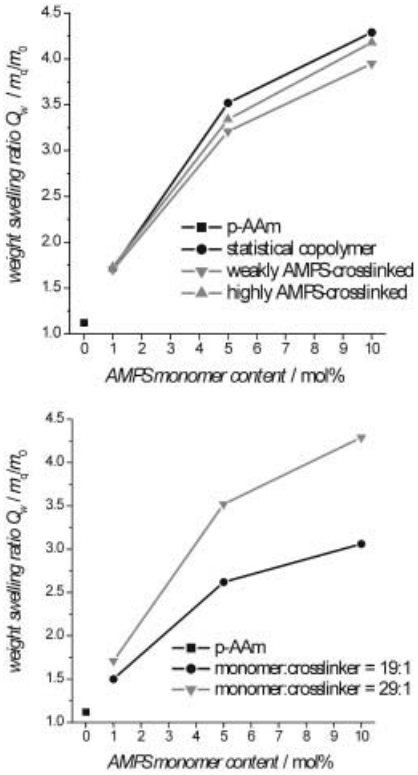


Figure 4. Top: Weight swelling ratios of AMPS copolymers with varying spatial arrangemnets of functional groups within the network. Bottom: Weight swelling ratio of copolymers with different monomer/cross-linker ratio.

**Mineralization of $CaCO_3$ in sulfonate bearing hydrogels**: Crystals obtained by counter diffusion experiments in AAm-AMPS copolymers have a characteristic morphology (Figure 5). After one week the experiments were terminated and aggregates of isometric habitus were isolated from the hydrogel. As confirmed by powder X-ray diffraction (XRD), the thermodynamically stable calcite modification of $CaCO_3$ is obtained. The size varies from 100 to 500 μm, dependent on the location within the hydrogel bodies. Calcite crystals closer to the $CaCl_2$ solution are smaller relative to those near the $NaHCO_3$ solution of the double-diffusion set-up.

Upon closer inspection with SEM, the aggregates do not show smooth faces as expected for pure calcite crystals. In contrast to these, the macrocrystals are composed of numerous calcite rhombohedra that build up a polyhedral aggregate. The orientation of rhombohedral "subcrystals" to the macrocrystal faces show strong similarities to calcite aggregates isolated from pure polyacrylamide (p-AAm) hydrogels.[10] The aggregates grown in p-AAm are composed of individual rhombohedral building blocks, leading to a pseudo-octahedral morphology of the macrocrystal. Both, aggregates obtained from crystal growth within the copolymer network, and p-AAm grown aggregates produce single-crystal X-ray diffraction patterns that correspond to distorted single crystals. Thus, the mineral tectonics and the structure of these macrocrystals is closely related.

While the calcite grown in p-AAm has a pseudo-octahedral habitus, the morphology of the aggregates isolated from the central part of AAm-AMPS copolymers resembles a cuboctahedron in which the vertices of the pseudo-octahedra are flattened. The crystallographic orientation of the flattened vertices is shown by SEM investigation of the macrocrystal surface (Figure 6). Terraces composed of crystal faces are

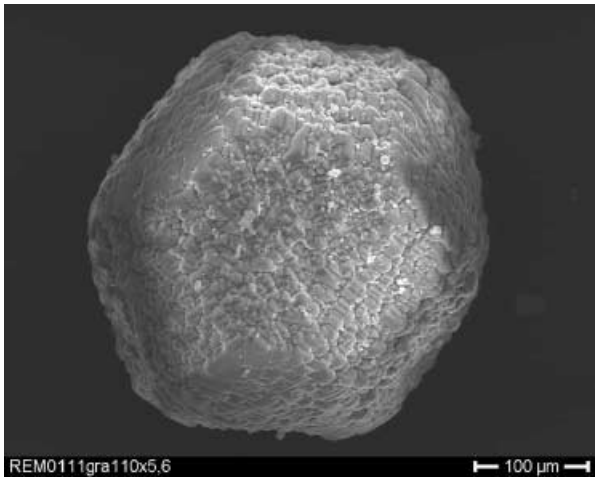


Figure 5. Micrograph of a pseudo-cuboctahedral aggregate crystallized within an AMPS copolymer containing 10 mol % sulfonate groups bearing monomers.

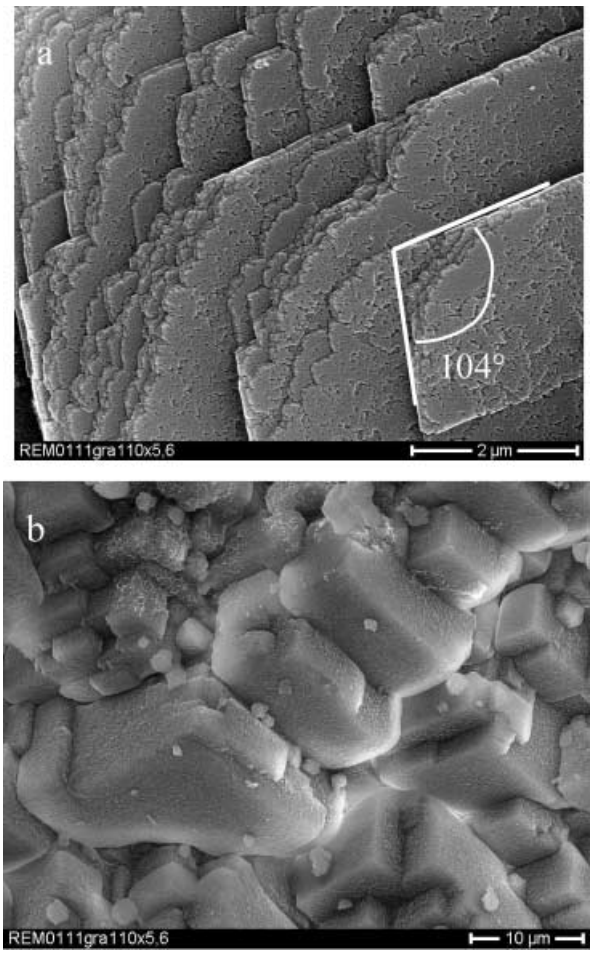


Figure 6. SEM images of the copolymer grown aggregate surface: a) Flattened vertices of pseudo-cuboctahedral particles showing calcite rhombohedra faces. b) Orientation of rhombohedral subcrystals on aggregate faces.

  0947-6539/03/0906-1313 $ 20.00+.50/0 

visible. As indicated in Figure 6a the angles between the edges amount to 104° and 76°, which correspond to those between the {10-14} faces of calcite. Another set of the pseudo-cuboctahedral faces is characterized by calcite rhombohedra vertices standing approximately perpendicularly (Figure 6b) to the macrocrystal faces, in analogy with the pseudo-octahedral faces of the p-AAm grown aggregates. As the Miller indices of the pseudo-octahedral faces were calculated in our previous paper, it is straightforward to describe the pseudo-cuboctahedra crystallographically. Utilizing the program JCrystal[17] the morphology is calculated with the {0001}, {01-11} (pseudo-octahedra faces), and {10-14} (flattened vertices) indices. The resulting habitus matches the observed pseudo-cuboctahedral morphology very well, as it can be seen by comparing Figure 7 and Figure 5. From the SEM investigations it can be concluded that the properties of aggregates grown in sulfonic acid based hydrogels are not fundamentally different from crystals grown in unfunctionalized p-AAm hydrogels.

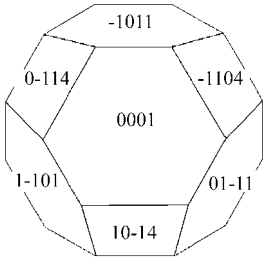


Figure 7. Schematic illustration of the pseudo-cuboctahedral morphology of calcite aggregates. The Miller indices of the corresponding calcite crystal faces are indicated. Compare with Figure 5.

**Crystal growth mechanism in sulfonate bearing hydrogels**: Comparison of crystals obtained from copolymers with increasing AMPS content reveals a pronounced change from the pseudo-octahedral towards a cuboctahedral morphology (Figure 8). Whereas the morphology of aggregates grown in copolymers with 1 mol% $-SO_3^-$ only slightly deviates from the pseudo-octahedral morphology, those obtained from copolymers with higher AMPS monomer content resemble a cuboctahedron. We suppose that the morphology is varied gradually, depending on the content of sulfonate groups within the copolymer. Due to the $-SO_3^-$-bearing functional groups the aggregate growth of the gel-grown particles is modified. Thus, the AMPS concentration of the copolymer network is a tool for fine-tuning the aggregate morphology.

For the aggregate growth of p-AAm grown pseudo-octahedra, it is supposed that the growth rate of {10-14} faces is enhanced owing to aggregation of preformed building blocks on the faces of a supercritical nucleus.[10] Therefore, the {10-14} faces dissappear during advanced aggregate growth. Since the AAm-AMPS-grown crystals have a pseudo-cuboctahedral morphology, composed of octahedral and rhombohedral faces, it seems that the growth rate of the {10-14} faces exceeds the growth rate of the octahedral faces to a lesser extent relative to the pseudo-octahedral growth.

The {10-14} form of calcite is the equilibrium morphology of calcite and results from crystal growth by ionic supply in diluted solutions.[18] In contrast to this, the pseudo-octahedra grown in p-AAm seem to be a consequence of aggregation of building blocks, which result from the reduced activation energy of nucleation in supersaturated solutions. Polar $-SO_3^-$ functional groups effectively immobilize $Ca^{2+}$ ions (comparable to ion exchangers[19]) leading to retarded diffusion. Consequently the concentration of $Ca^{2+}$ in the central part of the hydrogel body is decreased compared to double diffusion in unmodified p-AAm. The comparably moderate supersaturation leads to a hybrid crystal growth mechanism: Besides the aggregation of preformed building blocks, the {10-14} faces of calcite evolve due to ionic supply at near equilibrium crystallization conditions. Thus, the growth rate of the rhombohedral and octahedral faces are similar, resulting in a cuboctaheral morphology of the AAm-AMPS-grown aggregates.

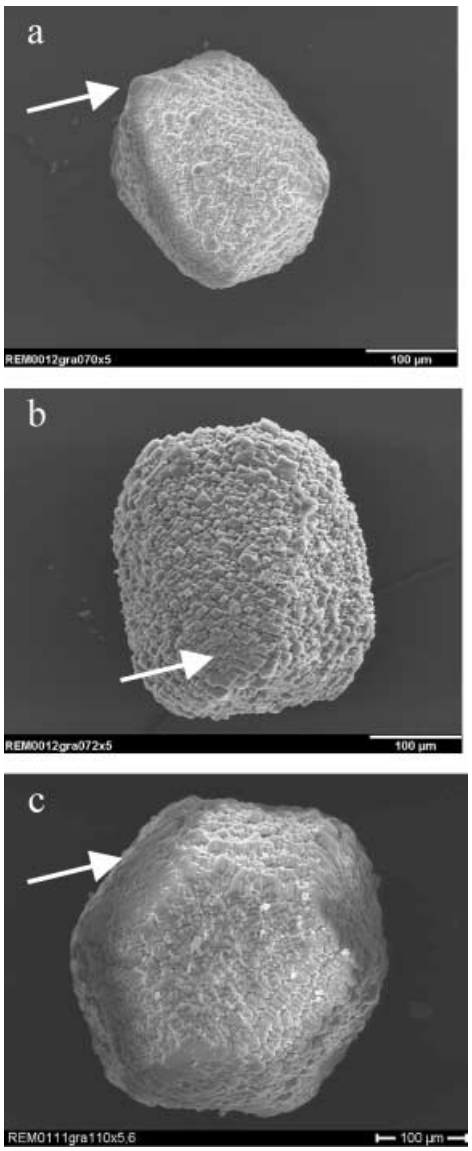


Figure 8. Micrographs of calcite aggregates crystallized in AMPS copolymers with an increasing content of sulfonate bearing monomers: a) 1 mol%, b) 5 mol%, c) 10 mol%. Arrows indicate the flatened octahedra vertices.



0947-6539/03/0906-1314 $ 20.00+.50/0 *Chem. Eur. J.* **2003**, *9*, No. 6

**Spatial distribution of sulfonate functional groups**: The morphologies of aggregates isolated from statistical and AMPS-cross-linked copolymers are similar. Consequently, the distribution of the AMPS functional groups within the network does not significantly affect the aggregate growth mechanism. However, the location of the particles within the hydrogel bodies, and the course of crystallization, is altered by the spatial arrangement of the AMPS functional groups. In Figure 9 photographs of the double-diffusion set-up are shown. Within AMPS-cross-linked copolymers first precipitation occurs near the $CaCl_2$ solution. In contrast to this, the first precipitation in a statistical AMPS copolymer (AMPS-1) takes place approximately in the middle of the gel bodies, and the time for the first crystallization is retarded.

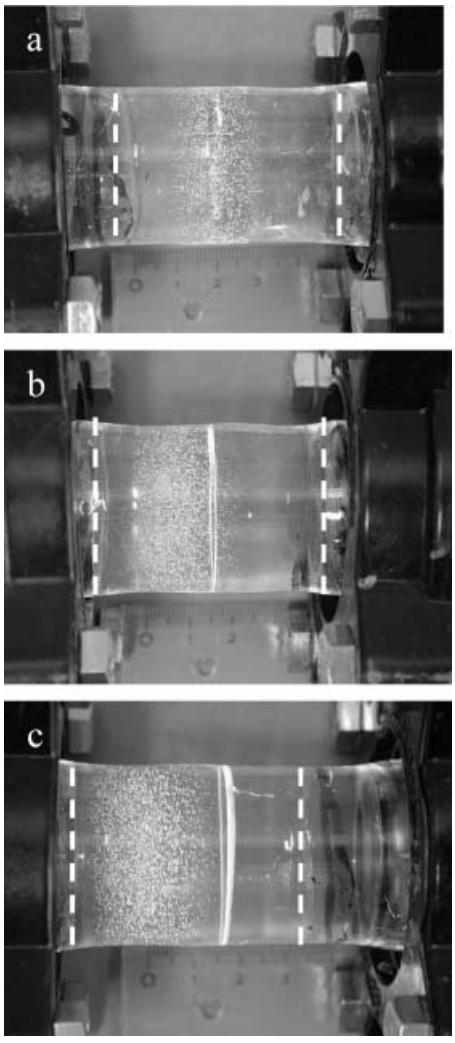


Figure 9. Photographs of hydrogel mounted in the double-diffusion set-up: $CaCl_2$ solution diffuses from the left, $NaHCO_3$ from the right; the sharp white ring results from manufacturing of the glass tubes. The boundaries of the hydrogels are indicated by dashed lines. a) statistical, b) weakly AMPS-cross-linked, and c) highly AMPS-cross-linked copolymer.

We suppose that the nucleation of calcite is affected by the spatial distribution of $-SO_3^-$ groups. Grouping of sulfonate functionalities in AMPS-2 and especially in AMPS-3 leads to local accumulation of $Ca^{2+}$. Thus, local enrichment of $Ca^{2+}$ will result in triggering the nucleation of calcite. A comparable mechanism is observed for the nucleation of ferrihydrite ($5\,Fe_2O_3 \cdot 9\,H_2O$) within ferritin proteins.[20] On the other hand, the statistical distribution of polar groups within AMPS-1 hydrogels inhibits the nucleation due to the immobilization and separation of $Ca^{2+}$. For that reason, the formation of critical nuclei is suppressed compared to copolymers with heterogeneous distribution of sulfonate groups.

## Conclusions

Whereas vinylsulfonate and allylsulfonate monomers are eluted from the corresponding polyacrylamido-copolymers, acrylamidomethylpropanesulfonate (AMPS) is covalently linked within the copolymer network. The $-SO_3^-$ content of this hydrogel is adjustable in the range from 0 to 20 mol%. The functional groups do not generally affect the aggregate growth mechanism of calcite, but modify the morphogenesis of the obtained crystals with respect to pure polyacylamide (p-AAm). By using p-AAm-AMPS copolymers with increasing amounts of $-SO_3^-$ groups, it is possible to fine-tune the morphology of the resulting aggregates. The local grouping of sulfonate groups within a hydrogel network results in unaltered morphologies with respect to copolymers with a random distribution of AMPS. The nucleation of calcite, however, is affected by the topography of the copolymers. We suppose that the crystallization of calcite is triggered by local accumulation of negatively charged nucleation sites. A comparable mechanism may promote the crystallization of various biominerals.

## Experimental Section

**Hydrogel synthesis**: The copolymerization of acrylamide monomers with sulfonate-containing monomers was based on the synthesis of pure polyacrylamide hydrogels.[10] Acrylamide (AAm, Fluka) and *N*,*N*′-methylenbis(acrylamide) (MBAAm, Aldrich) were dissolved together with either sodium vinylsulfonate (VlS, Aldrich), sodium allylsulfonate (AlS; ABCR), or 2-acrylamido-2-methyl-1-propane sulfonic acid (AMPS, Aldrich) in demineralized water (conductivity 0.055 μS). The cross-linking copolymerization was initiated with the radical starter ammonium-peroxodisulfate (APoxS, Aldrich), and the radical transmitter *N*,*N*,*N*′,*N*′-tetramethylethylene-diamine (TMEDA, Aldrich). The cross-linker ratio (mole ratio of cross-linker MBAAm to monomers AAm + (VlS, AlS, AMPS)) was fixed at 1:29 with an overall monomer concentration of 1.35 M. The content of sulfonate containing monomers (VlS, AlS, AMPS) of the polymerization mixture was varied from 0 to 20 mol% relative to the AAm monomers. Stock solutions of VlS, AlS and AMPS with concentrations of 0.1 M were prepared. The pH of the AMPS solution was adjusted by titration with 3 M NaOH solution to 7.0–7.4; the pH of VlS and AlS stock solutions amounted to 7.4 without further addition of NaOH. After mixing of the monomers, TMEDA and APoxS were added, resulting in concentrations of 10.1 mM and 1.8 mM, respectively, within the polymerization solvent. After addition of the starter, gelation of the copolymers occurred within 5 minutes. To ensure homogeneous polymerization throughout the gel bodies, the copolymers were placed in a drying chamber for 30 minutes and thereafter kept at ambient temperature for 48 hours. After ageing, the hydrogels were placed for four days into a 0.05 M solution of tris(hydroxymethyl)aminomethane, which was adjusted with a 2 M solution of HCl to a pH of 8.35 (Tris-HCl). Thereby the pH of the pore solution within the hydrogels was set to 8.35 and monomers not covalently linked to the network were eluted.

Besides the statistical copolymer (random distribution of the different monomer types; AMPS-1) described above, copolymers with a heterogeneous distribution of the AMPS monomer within the copolymer network were prepared. These hydrogels were synthesized in two steps (see flowcharts in Figure 10). For the "prepolymerization" AMPS stock solution

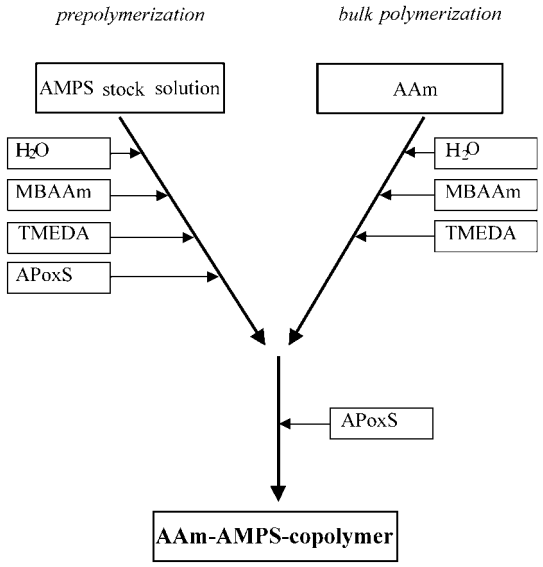


Figure 10. Flowchart of the polyacrylamide-*co*-acrylamidomethylpropanesulfonate copolymer synthesis with AMPS cross-linking.

was diluted with water and the cross-linker (MBAAm) was added. After complete dissolution of MBAAm the starter system was admixed to the AMPS-MBAAm monomer solution. By varying the amount of cross-linker during prepolymerization of AMPS, copolymers with different degrees of AMPS-cross-linking were obtained. Whereas for a weakly AMPS-cross-linked hydrogel (AMPS-2) the ratio AMPS/MBAAm amounted to 40:1, highly cross-linked copolymers (AMPS-3) had a corresponding ratio of 4:1. After adding APoxS the prepolymerization solution was agitated with a magnetic stirrer for 30 minutes. Simultaneous to the prepolymerization, AAm and MBAAm were dissolved in water ("bulk polymerization") and mixed with TMEDA. For reasons of comparability the total amount of cross-linker during synthesis was identical for the different copolymers. Thus less cross-linker was added to the bulk polymerization solution of AMPS-3 with respect to AMPS-2. After 30 minutes the AMPS-MBAAm monomer solution was poured into the bulk polymerization solution. The resulting solution was stirred for another 5 minutes before adding the remaining amount of radical starter. Gelation occurred within 5 minutes; ageing and elution with Tris-HCl was carried out analogously to the statistical polymerization.

**Hydrogel characterization**: To analyze the amount of sulfonic acid moieties covalently linked within the copolymer network, hydrogel portions (10 g) were eluted in demineralized water (50 mL). The hydrogels were not placed into Tris-HCl prior to elution. After 4 days the hydrogels were removed from the eluant, remaining water on the surface of the gels was removed with a blotting paper. Thereafter the eluted hydrogels were dried for 48 hours in an oven at 90 °C and ground by using an agate mortar. The sulfur content of the copolymers was determined by X-ray fluorescence analysis (XRF, Siemens SRS 3000) and compared to the initial sulfur concentration corresponding to the synthesis.

IR spectroscopy of dried copolymer samples was carried out with a Nicolet FT-IR 760 spectrometer. The potassium bromide (Aldrich, FT-IR grade) pellets contained 5 mass % xerogel and were prepared with a thickness of approximately 700 μm. The absorbances were calculated by using the baseline method.[11]

To examine the swelling behaviour of the AAm-AMPS copolymers, the hydrogel (10 g) was placed in demineralized water (250 mL) for 4 days. The gel plugs were weighed prior to incubation and immediately after swelling. At least two measurements of the weight swelling ratio were carried out to achieve good precision.

**Crystal growth**: The biomimetic crystallization of $CaCO_3$ was carried out by using a double-diffusion arrangement. The experimental set up was analogous to the one discribed in our previous paper.[10] The hydrogel plugs were placed into an U-shaped tube between aqueous solutions of buffered 0.1M $CaCl_2$ (Alfa Aesar) and 0.1M $NaHCO_3$ (Aldrich), respectively. The mineralization experiments were terminated after one week, and the $CaCO_3$ precipitates were separated from the hydrogel by oxidative decomposition of the organic matrix in a sodium hypochlorite solution (Riedel de Haen, 6–14% Cl active) and successive centrifugation.

The remaining inorganic phase was analyzed by powder X-ray diffraction (XRD; Stoe Stadi P) and scanning electron microscopy (SEM; Hitach S800). Single-crystal X-ray diffraction data were obtained by using a three-circle single-crystal diffractometer equipped with a CCD camera (Bruker AXS, SMART APEX-detector).

## Acknowledgement

This work was supported by the Deutsche Forschungsgemeinschaft (DFG) within the framework of the Schwerpunktprogramm (SPP) "Prinzipien der Biomineralisation". The authors thank G. Müller for helpful discussions, R. Neder for the close cooperation in the single-crystal diffraction experiments, and M. Bockmeyer for experimental support.

[1] S. Mann, *Biomineralization. Prinziples and Concepts in Bioinorganic Materials Chemistry*, Oxford University Press, **2001**.
[2] L. Addadi, S. Weiner, *Angew. Chem.* **1992**, *104*, 159–176; *Angew. Chem. Int. Ed. Engl.* **1992**, *31*, 153–169.
[3] A. Belcher, E. Gooch in *Biomineralization* (Ed.: E. Baeuerlein), Wiley, New York, **2000**, pp. 221–249.
[4] H. Lowenstam, S. Weiner, *On Biomineralization*, Oxford University Press, Oxford, **1989**.
[5] M. De Guire, H. Shin, R. Collins, M. Agarwahl, C. Sukenik, A. Heuer, *Proc. SPIE-Int. Soc. Opt. Eng.* **1996**, *2686*, 88–99.
[6] J. Aizenberg, A. Black, G. Whitesides, *J. Am. Chem. Soc.* **1999**, *121*, 4500–4509.
[7] P. Calvert, P. Rieke, *Chem. Mater.* **1996**, *8*, 1715–1727.
[8] H. Bekele, J. Fendler, J. Kelly, *J. Am. Chem. Soc.* **1999**, *121*, 7266–7267.
[9] E. Greenfield, D. Wilson, M. Crenshaw, *Am. Zool.* **1984**, *24*, 925–932.
[10] O. Grassmann, R. Neder, A. Putnis, P. Löbmann, *Am. Mineral.*, in press.
[11] M. Hesse, H. Meier, B. Zeeh, *Spektroskopische Methoden in der Organischen Chemie*, Thieme, Stuttgart, **1987**.
[12] Y. Kejun, Z. Guowei, *J. Appl. Polym. Sci.* **1992**, *44*, 1–7.
[13] S. Durmaz, O. Okay, *Polymer* **2000**, *41*, 3693–3704.
[14] M. Bockmeyer, unpublished results.
[15] P. Flory, *Principles of Polymer Chemistry*, Correll University Press, London, **1953**.
[16] H. Nottelmann, Ph.D. Thesis, Universität Hamburg, **1990**.
[17] JCrystalSoft, **2000**, version 1.02.
[18] P. Ramdohr, H. Strunz, *Klockmanns Lehrbuch der Mineralogie*, Enke, Stuttgart, **1967**.
[19] J. Sherman, *Adsorption and Ion Exchange: Progress and Future Prospects*, American Institute of Chemicals Engineers, New York, **1984**.
[20] V. Wade, S. Levi, P. Arosio, A. Treffry, P. Harrison, S. Mann, *J. Mol. Biol.* **1991**, *221*, 1443–1452.

Received: September 18, 2002 [F4437]

  